Micromineralogy of Galena Ores, Burgin Mine East Tintic District Utah

GEOLOGICAL SURVEY PROFESSIONAL PAPER 614-A

Micromineralogy of Galena Ores, Burgin Mine East Tintic District Utah

By ARTHUR S. RADTKE, CHARLES M. TAYLOR, *and* HAL T. MORRIS

SHORTER CONTRIBUTIONS TO GENERAL GEOLOGY

GEOLOGICAL SURVEY PROFESSIONAL PAPER 614-A

A study of the distribution of a variety of chemical elements in the major and minor minerals of a silver-rich lead and zinc replacement ore body

UNITED STATES GOVERNMENT PRINTING OFFICE, WASHINGTON : 1969

UNITED STATES DEPARTMENT OF THE INTERIOR

STEWART L. UDALL, *Secretary*

GEOLOGICAL SURVEY

William T. Pecora, *Director*

For sale by the Superintendent of Documents, U.S. Government Printing Office
Washington, D.C. 20402 - Price 40 cents (paper cover)

CONTENTS

ILLUSTRATIONS

[All illustrations are photomicrographs]

TABLES

MICROMINERALOGY OF GALENA ORES, BURGIN MINE, EAST TINTIC DISTRICT, UTAH

By Arthur S. Radtke, Charles M. Taylor, and Hal T. Morris

ABSTRACT

Analyses of argentiferous galena ores from the Burgin mine, Utah, by electron microprobe, emission spectograph, and wet chemical method indicate distinctly different amounts of silver in two general types of galena. Massive coarse-grained galena contains an average 0.22 percent silver by weight (approximately 64 ounces per ton), whereas fine-grained galena has less than 0.04 weight-percent silver (approximately 12 ounces per ton). The primary silver minerals dispersed in the galenas include polybasite, tetrahedrite, and jalpaite. Secondary silver sulfides, including argentite (or acanthite) and jalpaite, are concentrated in cerussite along fractures.

INTRODUCTION

The Burgin mine, in the East Tintic mining district, Utah, has recently become a major source of lead, zinc, and silver ores in an area that is widely known for rich and extensive replacement deposits (Lovering and Morris, 1960, p. 1116–1147; Bush and Cook, 1960, p. 1507–1540). The principal ore body in the mine, from which the samples described in this report were taken, is localized in sheared and brecciated rocks near the sole of the East Tintic thrust fault. This ore body is reported to contain more than 1,250,000 tons of ore with an average content of 10 ounces of silver per ton, 15 percent lead, and 12 percent zinc (Mining Congress Journal, 1961). Several times this amount of lower grade ore forms a casing around the high-grade ore body, and other ore bodies, estimated to contain an even larger quantity of medium- and low-grade ore, have been discovered nearby. In general, the ores consist of various proportions of argentiferous galena, sphalerite, pyrite, and minor quantities of other metallic minerals in a gangue of rhodochrosite and baritic jasperoid. These minerals replace brecciated masses of Cambrian limestone that have been overturned and thrust over argillaceous limestones of Ordovician age. All the Paleozoic rocks in the mine area are concealed beneath altered quartz latite lavas of Eocene age that postdate the structural events but predate ore deposition.

The two ore types described in this report are representative of two major varieties of lead ore in the central part of the main Burgin ore body. Samples of both were collected by H.T. Morris in November 1965 from the 1,200-foot level of the mine shortly after the main ore body was first reached on this level. Type 1 ore is massive coarse-grained galena which forms a lead-rich zone near the footwall of the deposit. Type 2 ore is somewhat finer grained galena that is intergrown with minor sphalerite near the hanging wall of the deposit. The contact between the two types of galena ore is abrupt and apparently indicates either a change in the composition of the ore solutions during deposition or postdepositional leaching and recrystallization of part of the ore body.

ACKNOWLEDGMENTS

The writers thank Mr. Gale Hansen, former mine superintendent, and Mr. William M. Shepard, mine geologist, for permission to sample the ore body of the Burgin mine. Dr. Victor Macres, President, Materials Analysis Co., generously permitted the use of Model 400 electron-beam microprobe analyzers and other facilities at the company laboratories in Palo Alto, Calif.

PURPOSE AND PROCEDURE

Examination of the galena ores from the Burgin mine was undertaken to (1) study the distribution of silver, (2) identify all ore and gangue minerals, (3) study textural and physical relationships of the minerals, and (4) study chemistry and element distribution of the minerals.

Mineral identifications were made by using the combined techniques of electron microprobe analysis, X-ray powder diffraction, and microscopy. The extremely small grain size of many of the phases necessitated extensive use of the electron microprobe analyzer. Sample preparation was done by Radtke and Taylor in the laboratories of the Materials Analysis Co., Palo Alto, Calif., and the U.S. Geological Survey, Menlo Park, Calif. All analytical work was done with Materials

Analysis Co. Model 400 two-channel and three-channel electron-beam microprobe analyzers.

Mineral textures and physical relationships were studied in polished section and, to a lesser extent, in hand specimen and are shown in numerous photomicrographs. The polished sections were made by mounting thin wafers of ore in epoxy casting resin set in stainless steel rings. The surfaces selected for study were ground, impregnated, and polished following the method described by Taylor and Radtke (1965). Use of the stainless steel mounting ring and careful sample preparation resulted in virtually no loss or plucking of galena and other minerals from the surface, as well as in extremely low relief between galena and quartz.

Bulk samples of the galena ores were analyzed by standard wet-chemical and spectrographic techniques. The chemical compositions of all minerals were determined with the electron microprobe analyzer. Certain aspects studied in detail include chemical zoning within minerals and element-concentration gradients across mineral boundaries. Numerous electron-beam scanning (EBS) X-ray images illustrate element distribution between and within phases.

Instrument geometry for the Materials Analysis Co. Model 400 electron-beam microprobe includes (1) electron incident angle, phi (ϕ) = 62.5°; (2) X-ray takeoff angle, theta (θ) = 33.5°; and (3) geometric factor for absorption corrections is $\csc(\theta)\cdot\sin(\phi)=1.6071$.

Operating potentials (excitation potentials) used in semiquantitative and quantitative analyses were 30 kv (kilovolts), zinc and copper; 25 kv, iron and manganese; 20 kv, indium, sulfur, cadmium, antimony, lead, silver, calcium, and chlorine; 15 kv, arsenic; 7 kv, oxygen. All electron-beam X-ray scanning images were made at 20 kv operating potential except oxygen, which was made at 7 kv. The $K\alpha$ characteristic lines were used for oxygen, silicon, sulfur, chlorine, calcium, iron, copper, and zinc; $L\alpha$ characteristic lines were used for arsenic, strontium, silver, cadmium, antimony, and barium; the $M\alpha$ characteristic line was used for lead.

Pure-element and compound standards used in the quantitative analyses included Fe, Cu, Zn, Ag, Cd, SiO_2, NaCl, GaAs, $SrSO_4$, $BaSO_4$, $PbCO_3$, PbS, and apatite. X-ray mass-absorption coefficients were taken from Heinrich (1966) and from unpublished data assembled by Metals Research, Ltd., Melbourn Royston Herts, England. In the reduction of electron microprobe X-ray intensity data, corrections were made for (1) drift in the incident electron-beam current; (2) background from the continuous spectrum; (3) absorption effects; and (4) atomic-number effects. Atomic-number and absorption corrections were taken from tables by Adler and Goldstein (1965), calculated from absorption corrections by Philibert (1963), and the Duncumb and Shields' (1966) overvoltage correction.

MINERALOGY AND CHEMISTRY

The first of the two types of ore, designated "type 1," is coarsely crystalline galena with thin coatings of secondary minerals. The second, designated "type 2," is massive fine-grained crystalline galena with minor amounts of sphalerite and abundant overgrowths of secondary minerals.

All minerals identified in the ore samples are listed with their compositions in table 1.

TABLE 1.—*Minerals in the galena ores of the Burgin mine*

Galena	PbS
Sphalerite	ZnS
Pyrite	FeS_2
Chalcopyrite	$CuFeS_2$
Tetrahedrite	$(Cu, Zn, Ag)_{12} (Sb, As)_4 S_{13}$
Polybasite	$(Ag, Cu)_{16} Sb_2 S_{11}$
Jalpaite	$Cu_{0.46} Ag_{1.54} S$
Silver sulfide*	Ag_2S
Lead–antimony oxide–carbonate	(Pb–Sb–C–O) †
Cerussite	$PbCO_3$
Calcite	$CaCO_3$
Mimetite	$Pb_5(AsO_4)_3 Cl$
Hematite	Fe_2O_3
Quartz	SiO_2
Barite	$BaSO_4$
Anglesite(?)	$PbSO_4$

*Acanthite or argentite.
†Precise composition not determined.

Small bulk samples of both type 1 and type 2 ores were crushed and ground for analysis. Chemical analyses for total lead and complete semiquantitative spectrographic analyses of galena ores are given in table 2.

GALENA

The coarsely crystalline galena of the type 1 ore contains small amounts of dispersed and associated gangue minerals, including quartz, barite, and calcite. Small rounded or oval grains of polybasite, tetrahedrite, and jalpaite are also dispersed through the galena; no acanthite or argentite was identified as primary inclusions or as exsolution blebs in the galena, and sphalerite is extremely rare.

In contrast to type 1, the fine-grained crystalline galena of the type 2 ore contains slightly greater amounts of quartz, barite, and calcite gangue minerals. Minor amounts of pyrite, tetrahedrite, and chalcopyrite are associated with the gangue minerals, and sphalerite is locally abundant. Compared with the coarse-grained type 1 galena, the fine-grained variety is relatively free of dispersed rounded grains or inclusions that are commonly attributed to exsolution. The most abundant inclusions are tetrahedrite. Jalpaite is minor, and no polybasite was noted.

TABLE 2.—*Chemical and spectrographic analyses of galena ores, Burgin mine*

[Spectrographic analyses by Chris Heropoulos. Values in weight percent]

Element	Massive coarsely crystalline galena (type 1)	Massive fine-grained crystalline galena (type 2)	Element	Massive coarsely crystalline galena (type 1)	Massive fine-grained crystalline galena (type 2)
Pb*	85.3	75.0	Ba	0.0007	0.2
Si	.05	2.0	Cd	.007	.03
Al	.005	.02	Cr	.00015	.0003
Fe	.005	.01	Cu	.02	.07
Mg	.0002	.0007	In	0	.005
Ca	.005	.01	Ni	.0005	.0005
Ti	0	.007	Sb	.5	.03
Mn	.0015	.0007	Sr	.005	.01
Ag	.2	.15	Zn	0	.5

*Determined by chemical gravimetric technique.

Note: Spectrographic results are reported in percent to the nearest number in the series 1, 0.7, 0.5, 0.3, 0.2, 0.15, 0.1, . . . , which represent approximate midpoints of interval data on a geometric scale. The assigned interval for semiquantitative results will include the quantitative value about 30 percent of the time. Tested for but not found in spectrographic analysis: Na, K, P, As, Au, B, Be, Bi, Ce, Co, Eu, Ga, Ge, Hf, Hg, La, Li, Mo, Nb, Pd, Pt, Re, Sc, Sn, Ta, Te, Th, Tl, U, V, W, Y, Yb, Zr.

The two types of galena show distinct differences in silver and antimony contents. The fine-grained galena does not contain detectable amounts of either silver or antimony in the mineral structure. The limit of detection for both elements in PbS by electron-beam microprobe analyses is 0.04 percent. In contrast, the coarsely crystalline galena has an approximate average content of 0.22±0.02 weight-percent silver and 0.25±0.02 weight-percent antimony. The value for silver is considerably higher than the 0.16 weight-percent reported by Taylor (1967) for galena-clausthalite associated with rich silver ores from Republic, Wash.

Small increases in both the silver and the antimony content in galena are apparent within 100 microns of polybasite inclusions. Such increases were not found within corresponding distances from the tetrahedrite inclusions. Other elements—such as copper, zinc, iron, cadmium, arsenic in tetrahedrite, and copper in polybasite—show no concentration in galena near these two minerals.

POLYBASITE

The small oval grains of polybasite dispersed in the massive coarsely crystalline galena of type 1 occur both singly and as a series of grains in a chainlike or linear orientation (fig. 1). The general composition of these grains in the galena host is given in table 3.

Polybasite is the antimony-rich end member in the polybasite-pearceite isomorphous series. In polished section under reflected light, it is pale brownish gray. The largest grains observed in the Burgin galenas are approximately 8 microns long and 4 mircons wide.

TABLE 3.—*Analyses of polybasite*

Element [1]	*Weight percent* [2]
S	12–16
Sb	10–14
As *	—
Cu	3–4
Ag	65–70

[1] Determinations by electron microprobe semiquantitative analysis.
[2] Values represent element abundance ranges.
* Arsenic tested for but not detected (<0.03). No other elements detected.

TETRAHEDRITE

Rounded or oval grains of tetrahedrite are dispersed through both types of galena (fig. 1) and also occur closely associated with gangue minerals in the fine-grained type 2 galena. All grains of tetrahedite analyzed contained small and varying amounts of silver, indicating that the variety in the Burgin ores should be designated as "silver-bearing tetrahedrite." Chemical analyses of tetrahedrite dispersed through galena and of tetrahedrite associated with gangue minerals show small variations in composition (table 4). A photomicrograph of a relatively large grain of tetrahedrite in galena is shown in figure 2.

TABLE 4.—*Analyses of tetrahedrite*

[Values, given in weight percent, represent element abundance ranges]

Element [1]	Dispersed in galena	With gangue in galena	Element [1]	Dispersed in galena	With gangue in galena
S	24–28	24–28	Fe	0.7	0.4
Sb	16–20	20–26	Ag	1.1–1.3	3.2–3.5
As	3.5–5	3–4	Cu	35–40	35–40
Cd	.5–.6	.6	Zn	6–6.5	6–6.5

[1] Determination by electron microprobe semiquantitative analysis. No other elements detected.

Chemical analyses of tetrahedrite show the ratio of antimony to arsenic, in weight percent, to be about 4–6 : 1. Tetrahedrite dispersed through galena compared with that associated with gangue contains consistently higher contents of arsenic and iron, and lower contents of antimony and silver (table 4). Preliminary studies show that the silver content in individual grains vary randomly up to the limits given in table 4; similar work was not done for other elements in tetrahedrite. Large amounts of zinc (6.0–6.5 percent) are present in the tetrahedrite and are accompanied by significant amounts of cadmium. Of the numerous tetrahedrite analyses listed by Palache, Berman, and Frondel (1944) none contain cadmium, which ranges to half a percent or more in the Burgin tetrahedrites.

Tetrahedrite in coarse-grained type 1 galena commonly occurs in relatively large (20–30 micron) grains. In contrast, tetrahedrite grains in fine-grained type 2 galena are much more numerous and much smaller (<1–2 microns in diameter). Under reflected light tetrahedrite in these ores is pale gray.

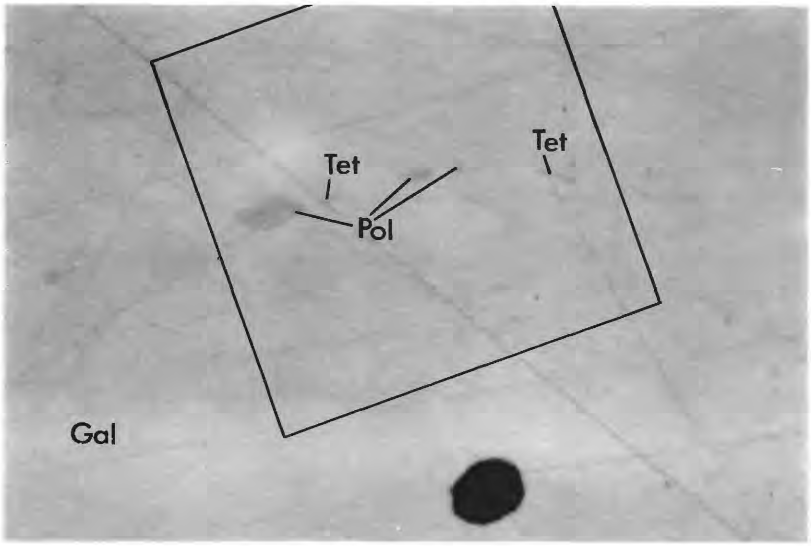

◀FIGURE 1.—Chainlike series of polybasite (Pol) and tetrahedrite (Tet) inclusions in galena (Gal). In general, inclusions of these two minerals in galena show no preferred orientation. Magnification × 445. *A–D*, X-ray scanning images for Sb, Ag, Cu, and Pb in the area outlined in figure 1. The symbols in the lower left-hand corner indicate the element represented by the bright areas of the photograph. Magnification × 650.

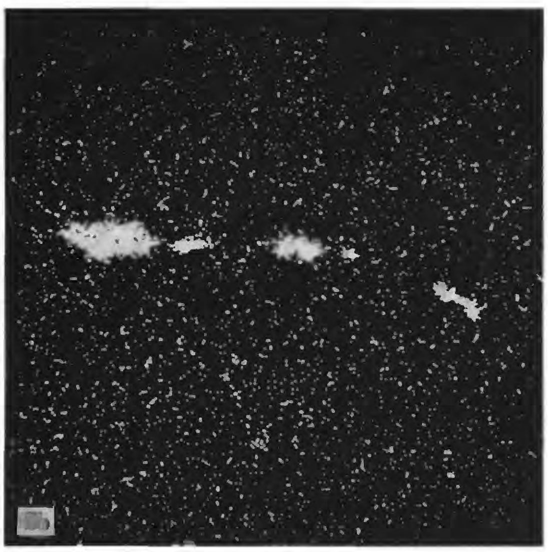

◀*A*

B▶

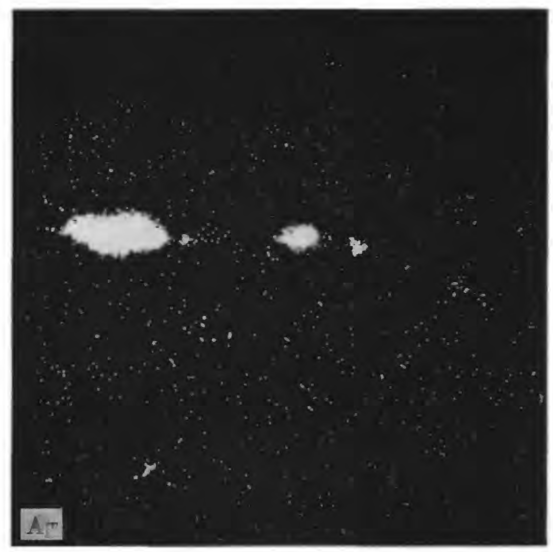

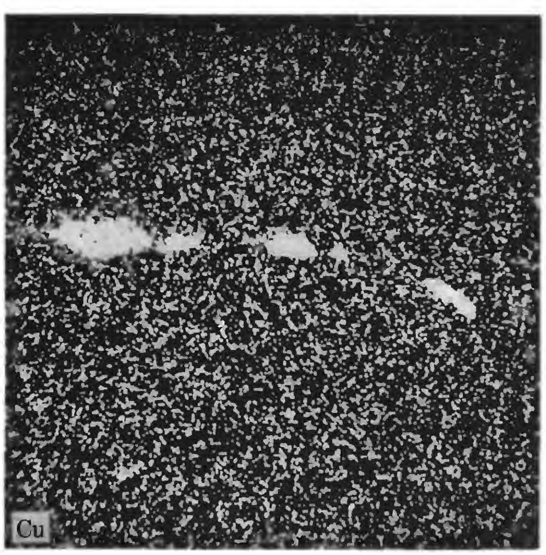

◀*C*

D▶

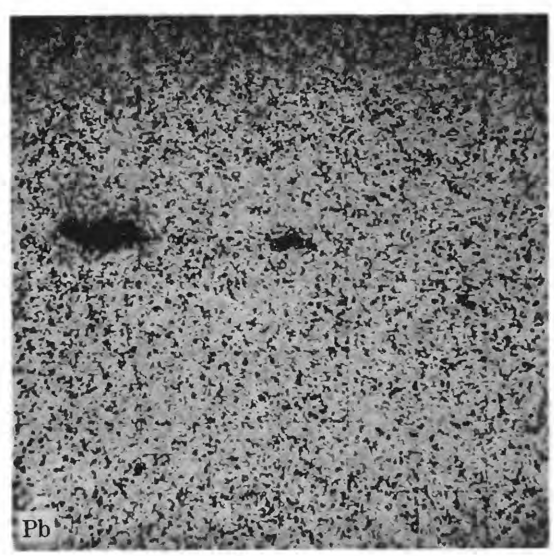

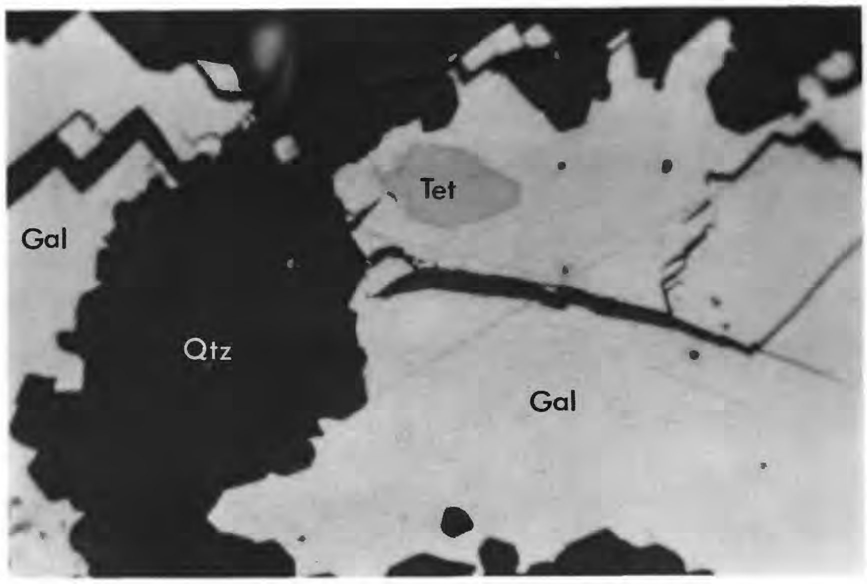

FIGURE 2.—Large grain of tetrahedrite (Tet) locked in fine-grained galena (Gal). Dark-gray phase is quartz (Qtz) gangue, and dark band along top of figure is mounting resin. Magnification × 330. Chemical data on this large tetrahedrite grain are given in table 4.

JALPAITE

Minor amounts of primary jalpaite were identified in coarse-grained type 1 galena as small clusters of round grains or inclusions (fig. 3). Although not closely associated with tetrahedrite, jalpiate is commonly present in and near areas of significant amounts of tetrahedrite. (See fig. 4.) The mineral is also secondary in origin and occurs in small grains (<1–2 microns in diameter) scattered through cerussite. Chemical analysis of jalpaite is given in table 5. The formula for jalpiate, as reported by Skinner (1966), is $Cu_{0.45}Ag_{1.55}S_{1.00}$ or $(0.45Cu_2S \cdot 1.00Ag_2S)$, having a cation to sulfur ratio of 2:1. From the analysis given in table 5 for copper and silver, and by calculating the atomic ratios and normalizing the cations to 2.00, the formula for jalpaite in Burgin ores is $Cu_{0.46}Ag_{1.54}S_{1.00}$ or $(0.46Cu_2S \cdot 1.54Ag_2S)$.

TABLE 5.—*Analysis of jalpaite*

Element [1]	*Weight percent*
S	15.5±0.5
Ag	72±1
Cu	12.5±0.2
Total	100.0

[1] Determinations by electron microprobe quantitative analysis. No other elements detected.

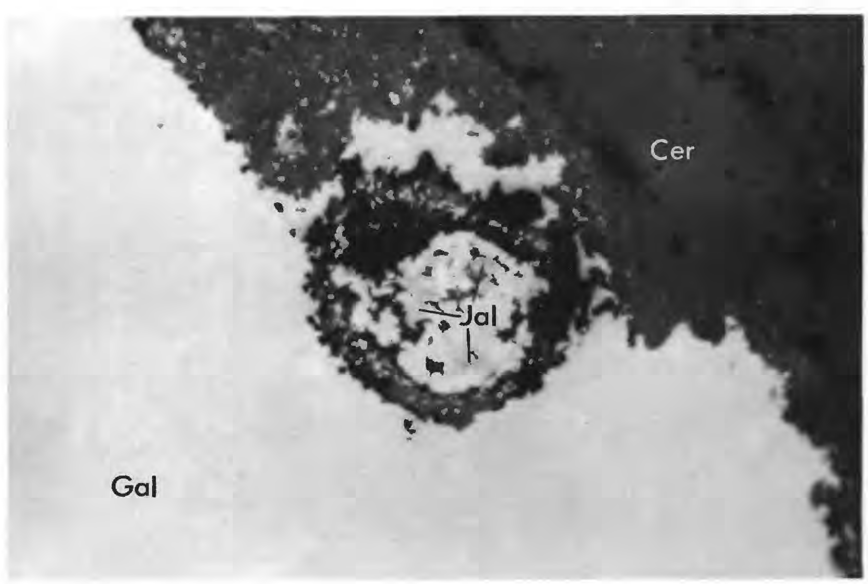

FIGURE 3.—Granular intergrowth of jalpaite (Jal) and galena (Gal) surrounded and replaced by cerussite (Cer). Fine-grained fragments in cerussite are remnant galena (Gal). Magnification × 645.

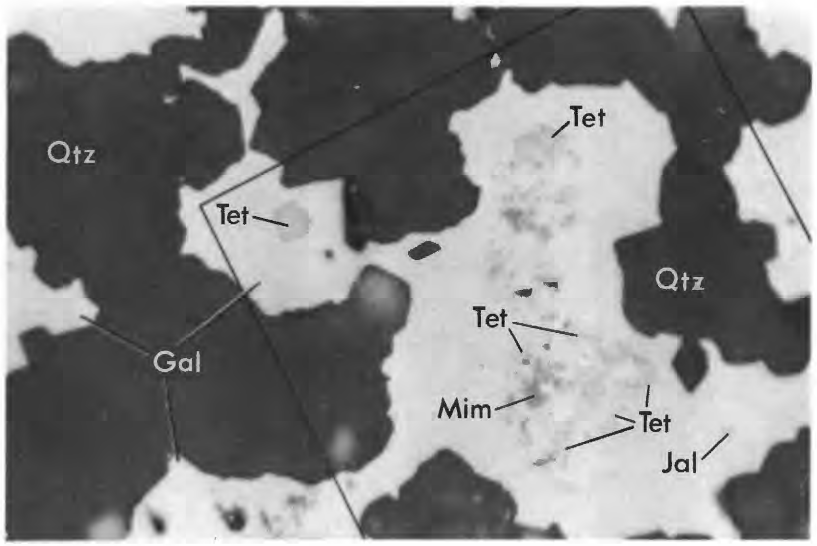

FIGURE 4▲

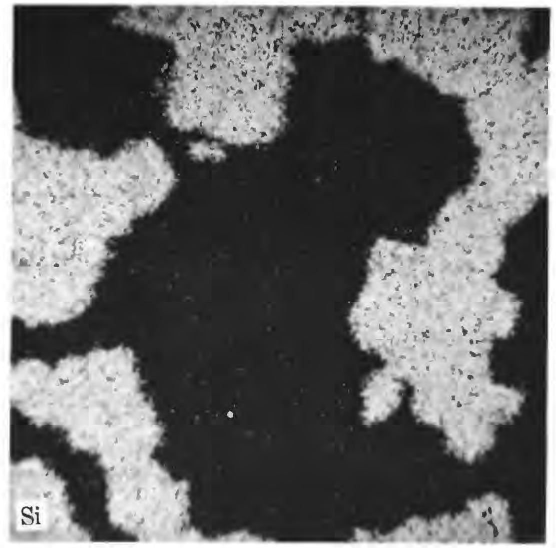

A▲

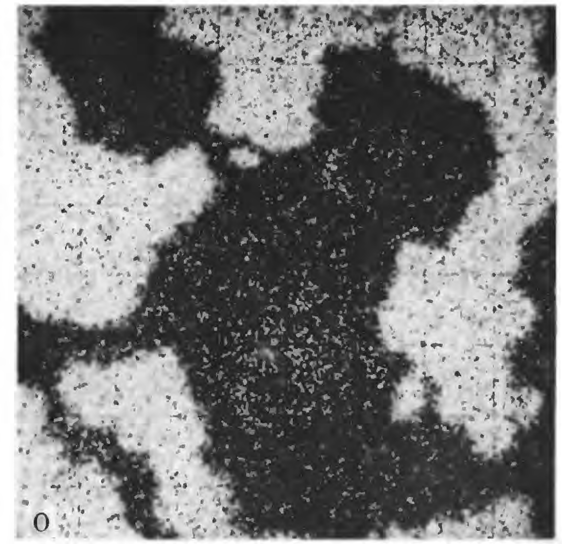

B▲

C▼

D▼

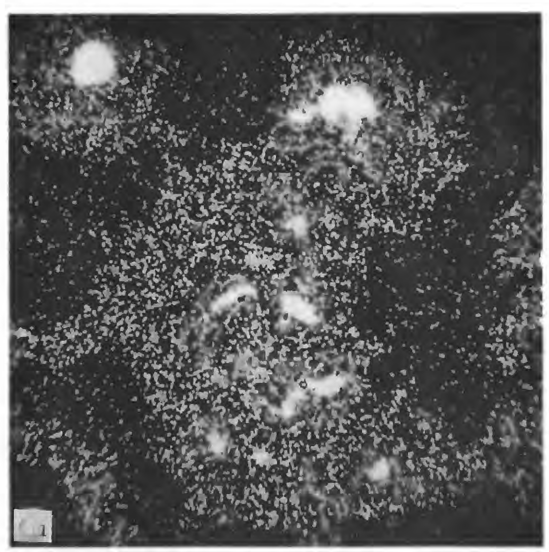

E▼

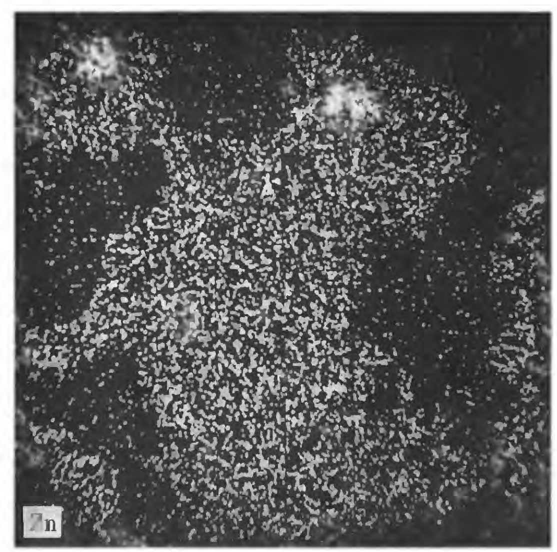

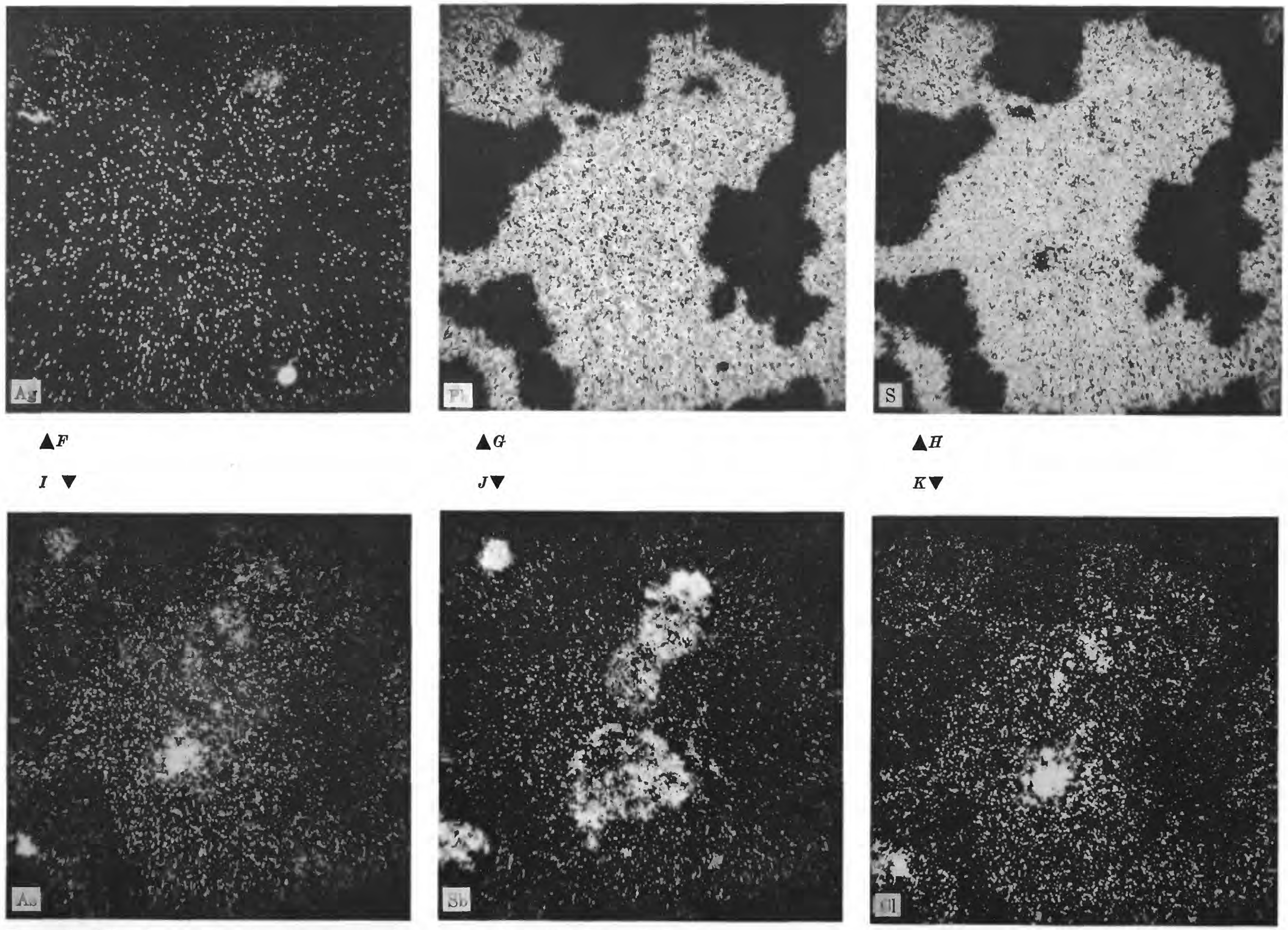

FIGURE 4.—Mimetite (Mim) forming along a microfracture in galena (Gal). Large dark areas are quartz (Qtz) gangue. Two large grains of tetrahedrite (Tet) and one small jalpaite (Jal) grain are locked in galena. Note two areas of microintergrowths in galena on right side of photograph. In these areas the darkest phase is mimetite, the lighter gray phase is tetrahedrite, and another gray phase (slightly darker than tetrahedrite) is a lead-antimony oxide or carbonate. Magnification × 330. *A–K*, X-ray scanning images for Si, O, Fe, Cu, Zn, Ag, Pb, S, As, Sb, and Cl in the area outlined in figure 4. The symbols in the lower left-hand corner indicate the element represented by the bright areas of the photograph. Magnification × 400.

LEAD-ANTIMONY OXIDE OR CARBONATE

An unknown secondary mineral containing large amounts of lead, antimony, and oxygen, plus a significant amount of iron, is closely associated with mimetite in the ore. Although the mineral is present in both types of galena ore, it is much more abundant in the fine-grained ore. In the massive coarse-grained galena ore, it is confined to, and dissemintaed through the cerussite coatings on galena. In the fine-grained galena ore, too, the mineral is confined to, and dispersed in, cerussite coatings on galena but is also common with mimetite and cerussite along microfractures in the galena (fig. 4) and as a thin (<1 micron) selvage between quartz grains and galena. Although the mineral is abundant, it everywhere is present only as particles 2–4 mircons in diameter.

Detailed quantitative electron microprobe study indicates that the mineral contains approximately 40 percent lead, 22 percent antimony, 2.2 percent iron, and 0.4 percent calcium. Sulfur is not present, and wavelength-shift studies on $S_{k\alpha}$ show no sulfate (SO_4^{-2}) to be present near the mineral. Behavior of the mineral under electron bombardment strongly suggests that it is anhydrous. Since the antimony, lead, iron, and calcium contents, when converted to oxides, are considerably less than 100 percent, and the mineral is confined to cerussite or a system rich in CO_3^{-2} molecule, it seems likely that the carbonate, or bicarbonate, is present. If the mineral is a carbonate, a general formula close to the following would be reasonable on the basis of known data:

$$3(Pb,Fe,Ca)CO_3 \cdot Sb_2O_3, \text{ or}$$
$$3(Pb,Fe,Ca)(HCO_3)_2 \cdot Sb_2O_3$$

The small particle size and interference from carbon and oxygen in cerussite surrounding the mineral prevented accurate carbon and oxygen analyses.

SPHALERITE

Sphalerite was not observed in the coarse-grained type 1 ore, but it is abundant as small grains interlocked within galena in the fine-grained type 2 ore. Locally, it is concentrated with quartz and barite, commonly rimmed by galena, which clearly replaces the earlier sphalerite crystals (fig. 5).

Chemical analyses of sphalerite grains are given in table 6. Numerous analyses were made on sphalerite grains, and the general discussion on composition of sphalerite given here incorporates data obtained from all analyses on the samples studied.

TABLE 6.—*Analyses of sphalerite*

Element [1]	*Weight percent* [2]	*Element* [1]	*Weight percent* [2]
S	30 –35	Cd	0.5 – 1.0
Zn	60 –70	In	.02 – .3
Fe	<.02– .07	Cu	.09

[1] Determinations by electron microprobe semiquantitative analysis. No other elements detected.
[2] Values represent element abundance ranges.

Continuous quantitative analyses for iron, cadmium, and indium were made along traverses across numerous sphalerite grains. The concentration of iron in most of the sphalerite grains is below the limit of detection (0.02 percent). The maximum amount found was 0.07 percent, but the minor concentrations apparently vary widely between grains and even within individual grains. In all the traverses the cadmium content varied directly with that of iron, and the maximum amount of cadmium found, 1.0 percent, was in the area

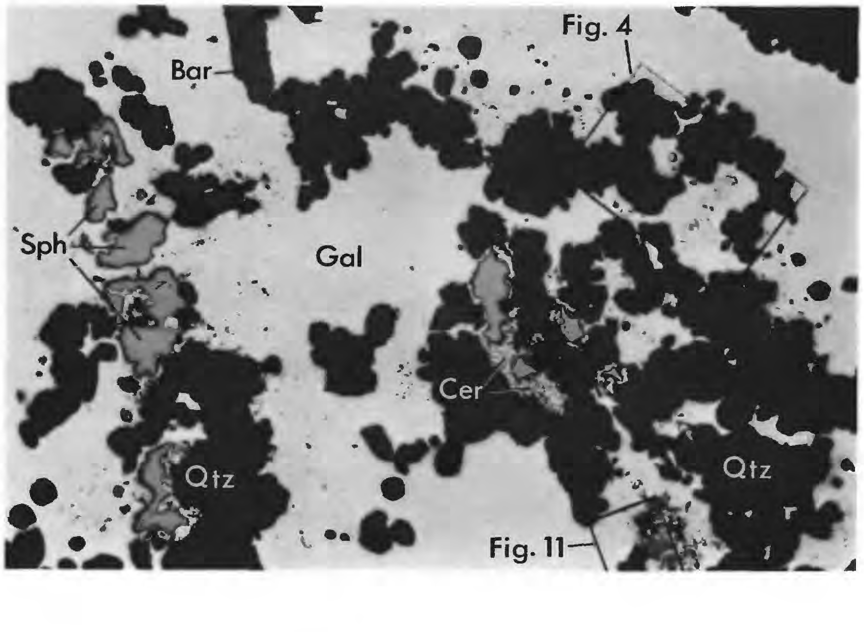

FIGURE 5.—Replacement of remnant grains of sphalerite (Sph), quartz (Qtz), and barite (Bar) by galena (Gal). Note alteration of galena to cerussite (Cer) near center of figure. The mineralogy and chemistry of microintergrowth areas in galena, outlined in the figure, are shown in detail in figures 4, 4A–K, and 11, 11A–K. Mimetite formed along microfractures is present in both outlined areas. Magnification ×80.

containing 0.07 percent iron. In contrast, the distribution and abundance of indium in sphalerite does not correspond to that of iron or cadmium. The highest indium content found was 0.3 percent, and the average is estimated to be 0.04 percent. Other elements specifically tested for in sphalerite but not found include silver, manganese, mercury, tin, gallium, and thallium.

Of particular interest is the cathodoluminescence of the sphalerite in the Burgin ores, which is apparently dependent on the minor element content. Under high-energy electron bombardment, the cadmium-bearing sphalerite emits radiation in the visible spectrum range that apparently varies with the concentration of cadmium in the following way: (1) >0.08 percent Cd, faint yellow white; (2) 0.05–0.07 percent Cd, faint greenish yellow; (3) 0.03–0.05 percent Cd, pale blue; (4) <0.03 percent Cd, pale red.

Since the iron content varies directly with the cadmium content, these color variations may also reflect small differences in the abundance of iron. Other elements considered to influence cathodoluminescence in sphalerite, such as manganese, may affect it. However, if present, such elements occur in amounts below the limit of detection in the samples studied.

PYRITE AND CHALCOPYRITE

Rare grains of both pyrite and chalcopyrite are present in the fine-grained type 2 ore, but are absent in the coarsely crystalline type 1 ore. Both minerals commonly occur in grains less than 10 microns in length. (See fig. 6.) No complete chemical analyses were made on these phases.

MIMETITE

Mimetite in small amounts was also identified in type 2 ore. It occurs with cerussite, minor amounts of anglesite(?), and calcite as a coating or overgrowth on galena. Commonly, it fills minor voids between the quartz or barite grains and the galena (fig. 7), as well as the microfractures within galena (fig. 4). Other secondary minerals commonly associated elsewhere with mimetite, such as smithsonite, hemimorphite, and wulfenite, were not identified. Their absence may reflect the general low abundance of iron, zinc, vanadium, and copper in the galena ores. The general low abundance of mimetite in the ore also doubtless reflects the low concentration of arsenic in the Burgin galena ores.

A complete chemical analysis of mimetite in the Burgin ores is given in table 7.

TABLE 7.—*Analysis of mimetite*

Element [1]	*Weight percent*
Pb	69 ±2
Ca	.4± .1
As	15 ±1
Cl	2.8± .2
O	13 ±2
Total	100.2

[1] Determinations by electron microprobe quantitative analysis. No other elements detected.

CERUSSITE

Large amounts of cerussite are present in both types of ore, both as surface coatings and along fractures and cleavage directions in galena. The cerussite commonly contains intergrowths of mimetite, jalpaite, secondary silver sulfide, secondary lead-antimony oxide or carbonate, and minor amounts of hematite, calcite and anglesite(?). The typical alteration of galena to cerussite along galena cleavage planes is shown in figure 8. Even in areas where this alteration is massive and virtually complete, numerous small inclusions of remnant galena remain. Although minor amounts of anglesite may be

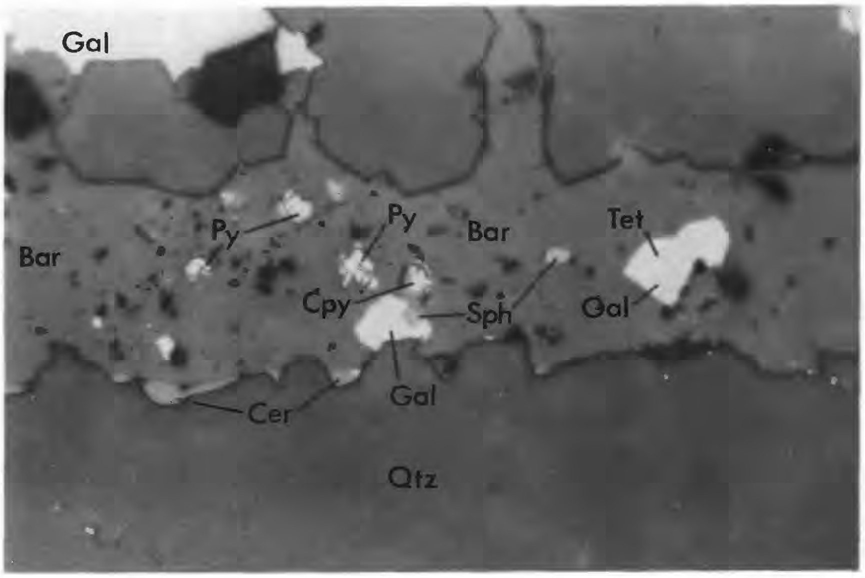

FIGURE 6.—Veinlet of late(?) barite (Bar) containing fragments of pyrite (Py), chalcopyrite (Cpy), sphalerite (Sph), and galena (Gal) cutting across quartz (Qtz). Note tiny inclusions of tetrahedrite (Tet) and sphalerite in galena fragments, and cerussite (Cer) along margin of veinlet. Magnification × 330.

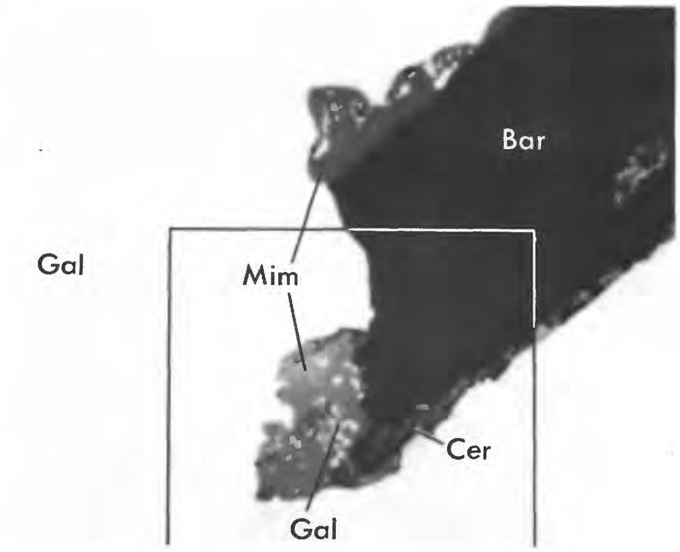

◀FIGURE 7.—Mimetite (Mim) along contact between galena (Gal) and barite (Bar) gangue. Small amounts of cerussite (Cer) are also present. Small white grains in mimetite are remnant galena grains. Magnification × 1,290. *A–F*, X-ray scanning images for Cl, As, O, Ba, Pb, and S in the area outlined in figure 7. The symbols in the lower left-hand corner indicate the element represented by the bright areas of the photograph. Magnification × 1,500.

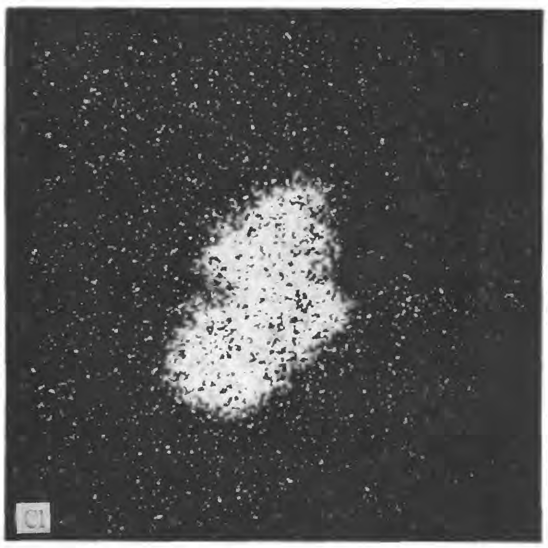

◀*A*

B▶

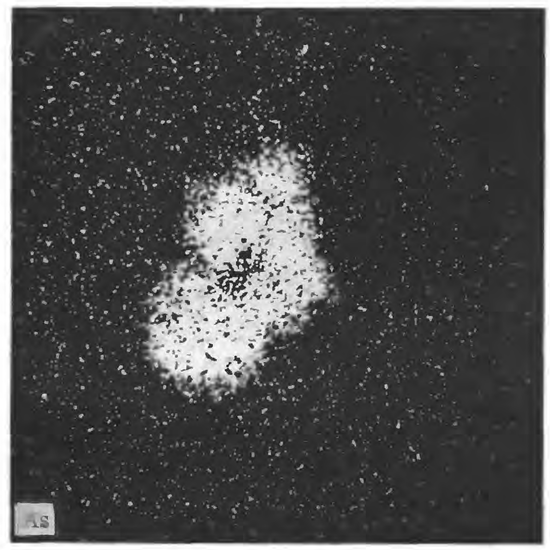

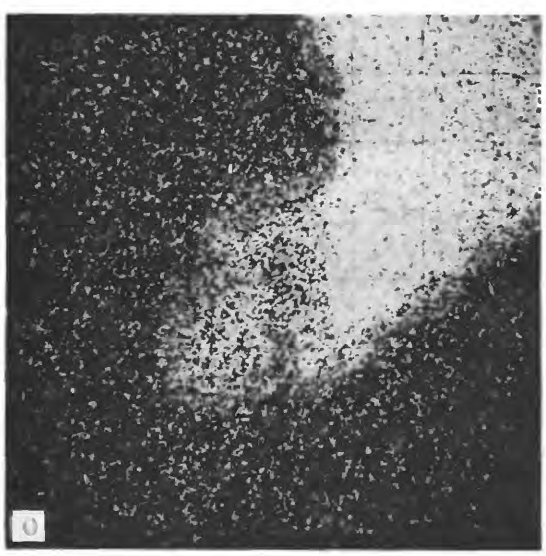

◀*C*

D▶

◀*E*

F▶

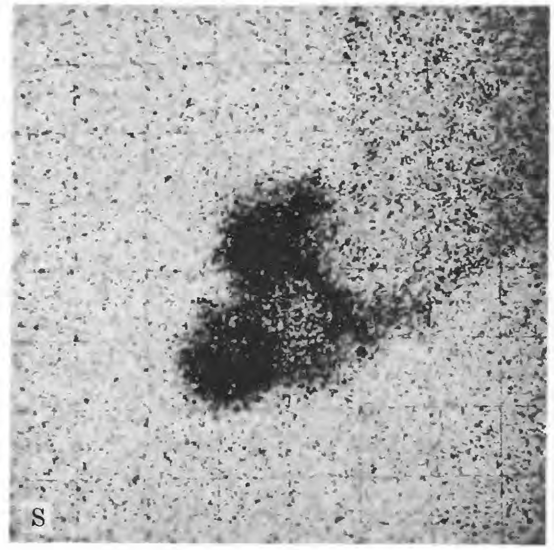

present with cerussite, no typical intermediate zone of lead sulphate was observed between the lead carbonate and the lead sulfide.

SILVER SULFIDE

Large amounts of argentite or acanthite of secondary or supergene origin containing minor amounts of copper (0.5–0.8 weight-percent Cu) are admixed with, and dispersed through, cerussite (fig. 9). The extremely small size of individual silver sulfide grains (<1–2 microns) precluded obtaining either the optical data or the X-ray diffraction data necessary for positive identification. Aggregates of granular grains that formed contemporaneously with cerussite are shown in X-ray scanning images (fig. 9*A*–*E*).

No primary argentite (or acanthite) was identified with the galena either as an individual intergrown mineral or in dispersed rounded exsolution-type grains.

HEMATITE

Minor amounts of hematite are present with cerussite in areas of extensive alteration of galena to the lead carbonate. The low abudance and erratic distribution of hematite reflects the corresponding occurrence of primary iron-bearing sulfides. X-ray scanning images for oxygen (fig. 11*B*) and for iron (fig. 11*C*) show the close association between hematite, cerussite, and the other alteration products.

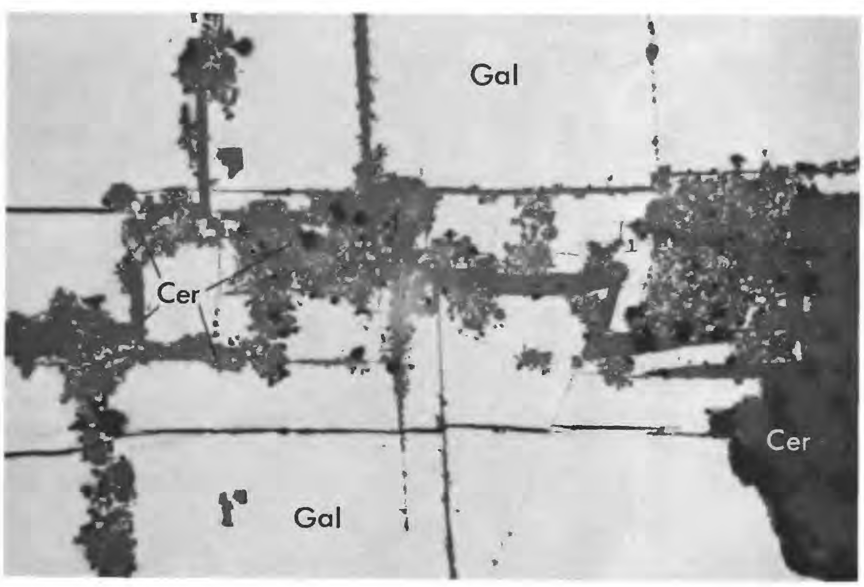

FIGURE 8.—Alteration of galena (Gal) to cerussite (Cer) localized along cleavage planes. Note remnant galena grains in cerussite. Small black spots are micropits produced in sample preparation. Magnification × 80.

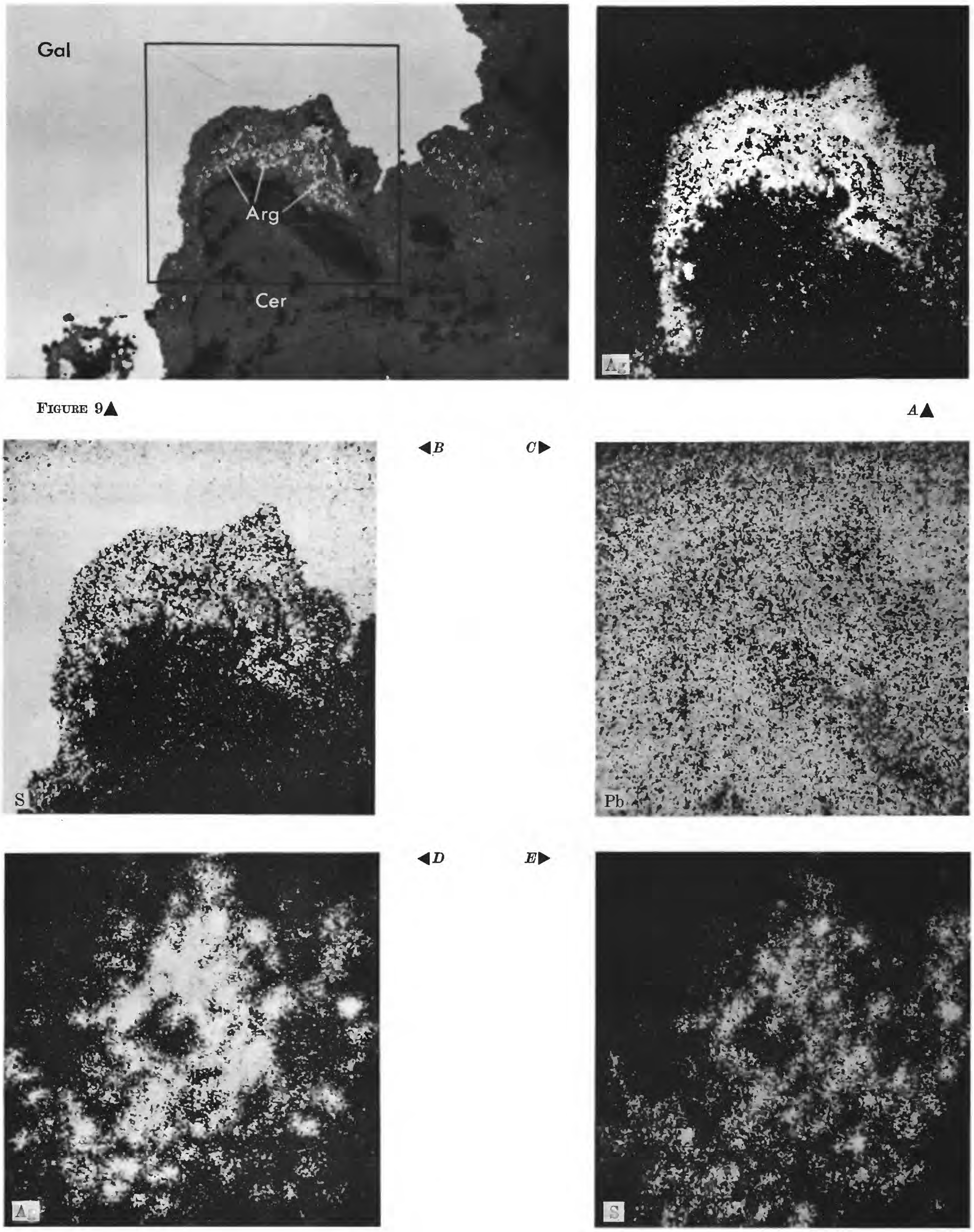

FIGURE 9.—(Explanation on next page.)

CALCITE AND ANGLESITE(?)

Minor amounts of both calcite and anglesite(?) are present with cerussite in both types of ore in areas where alteration of galena to cerussite is relatively complete. The calcite is commonly associated with mimetite and anglesite(?). As previously noted, anglesite is not concentrated along galena-cerussite contacts.

BARITE AND QUARTZ

Small amounts of barite and quartz form the gangue minerals in fine-grained type 2 ore. Only a few scattered grains of each were recognized in coarse-grained type 1 ore. Both minerals are dispersed through galena, and textural evidence clearly shows replacement of the early gangue minerals by galena (figs. 5, 10). The elongated and segmented appearance of barite crystals shown in figure 10 is common in the fine-grained ore. Barite generally occurs with quartz, although the reverse is not necessarily true.

Small veinlets of barite cutting galena and quartz suggest a second generation of late postore barite. These veinlets commonly contain numerous fragmental inclusions of early sulfide minerals (fig. 6).

ELEMENT DISTRIBUTION

Electron-beam scanning techniques allow graphic portrayal of the distribution of many key elements in the galena ores. These EBS X-ray scanning images are presented throughout the report.

Silver.—In the primary minerals silver is present in polybasite jalpaite, and tetrahedrite, although in tetrahedrite the silver content is far below the 17–19 percent apparent maximum level for freibergite. The two types of galena contain different amounts of silver. In areas near the polybasite inclusions, silver occurs as a small but definite concentration. Argentite, commonly reported to be intergrown with, or dispersed in, "silver-bearing galena," was not identified in the galena of the samples studied. Jalpaite and argentite (or acanthite) of supergene or secondary origin apparently formed with cerussite. This is particularly evident in figure 9 and in the X-ray scanning images for silver, sulfur, and lead distributions in figure 9*A–E*. A minimum of 50 percent of the total silver in the samples studied was represented by this latter occurrence.

Antimony.—The distribution and concentration of antimony in primary minerals in the ore is similar to that of silver with antimony concentrated in polybasite and tetrahedrite and in coarse-grained galena. The distribution of antimony, silver, copper, and lead between polybasite and tetrahedrite locked in galena are shown in X-ray scanning images (fig. 1*A–D*).

During oxidation and alteration of galena, antimony is concentrated in the secondary lead-antimony oxide or carbonate phase in cerussite. No antimony is present in the cerussite itself, with the limit of detection for antimony in lead carbonate of 0.04 percent.

Copper.—The minor amount of copper in primary sulfide ores is closely associated with silver and antimony in polybasite and tetrahedrite, and associated with silver in jalpaite. Only trace amounts of chalcopyrite were observed, and no simple sulfides of copper were recognized. The paucity of secondary or supergene copper minerals reflects the apparent general low abundance of copper compared with lead in the ore body. Jalpaite, the silver copper sulfide, was the only secondary copper mineral identified. The concentration of copper in sulfosalt minerals in galena is shown in X-ray scanning images (figs. 1*C*, 4*D*, 11*D*).

FIGURE 9.—Fine-grained secondary silver sulfide (Arg) dispersed in secondary cerussite (Cer). Note argentite or acanthite concentrated in narrow zone between galena (Gal) and inclusion-free cerussite. Black areas are micropits in cerussite. Magnification × 160. *A–C*, X-ray scanning images for Ag, S, and Pb in the area outlined in figure 9, Magnification × 240. *D* and *E*, X-ray scanning images for Ag and S at high magnification, showing typical fine-grained (<2 microns) silver sulfide dispersed through the lead carbonate matrix. Magnification × 1,300.

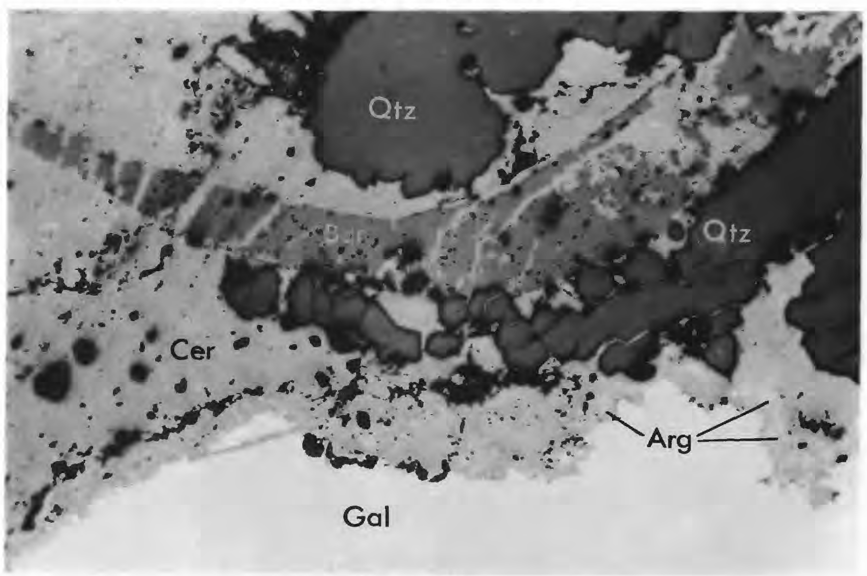

FIGURE 10.—Replacement of remanant quartz (Qtz) and segmented barite (Bar) by galena (Gal), which was subsequently altered to cerussite (Cer). Small white grains in cerussite are remnant galena and secondary silver sulfide (Arg). Magnification × 80.

FIGURE 10

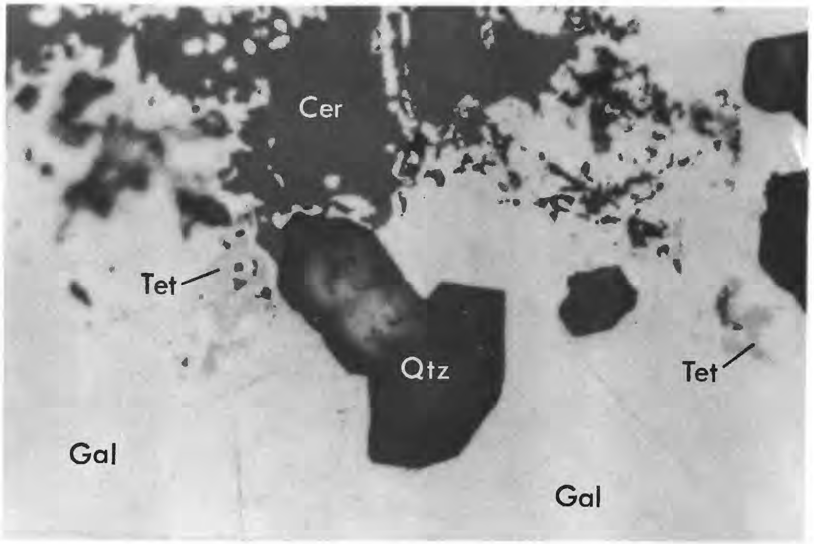

FIGURE 11▲

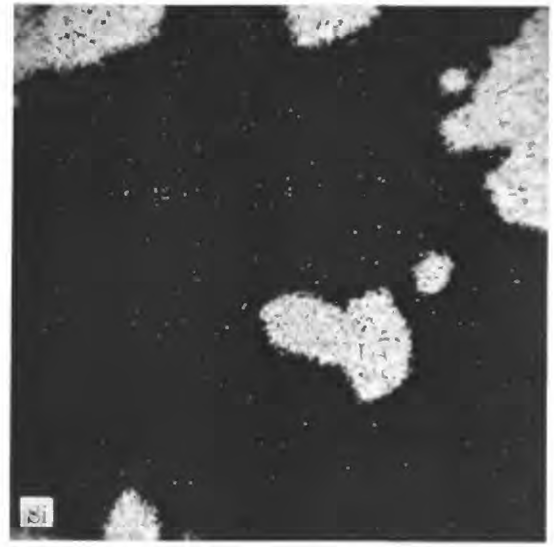

A▲

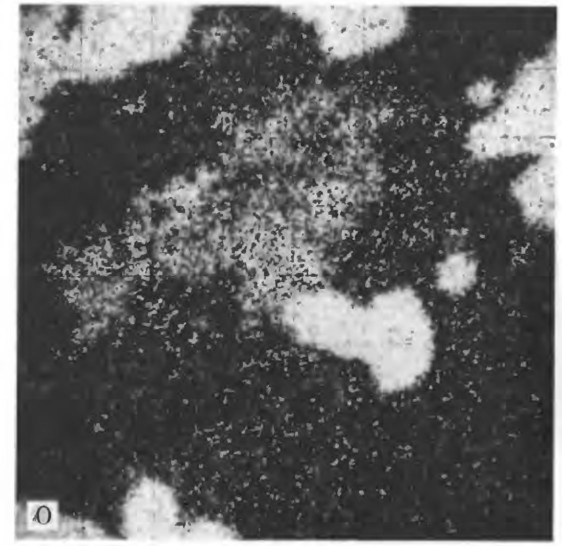

B▲

C▼

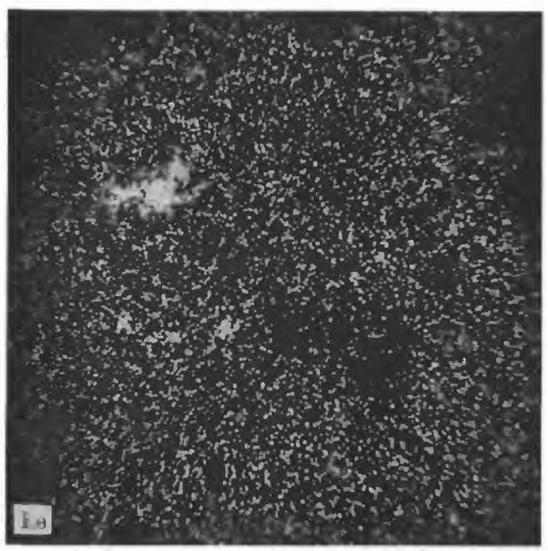

D▼

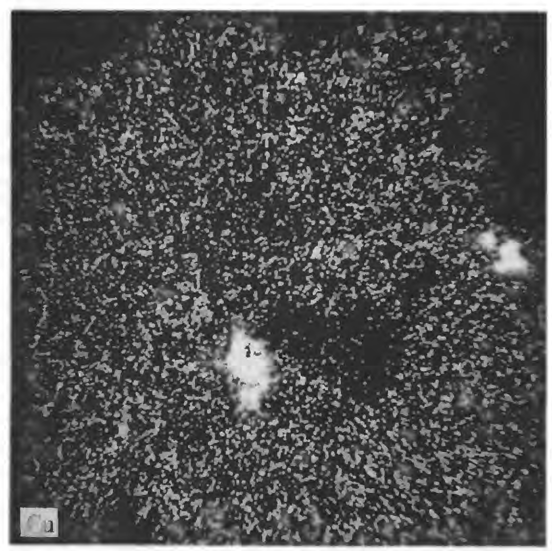

E▼

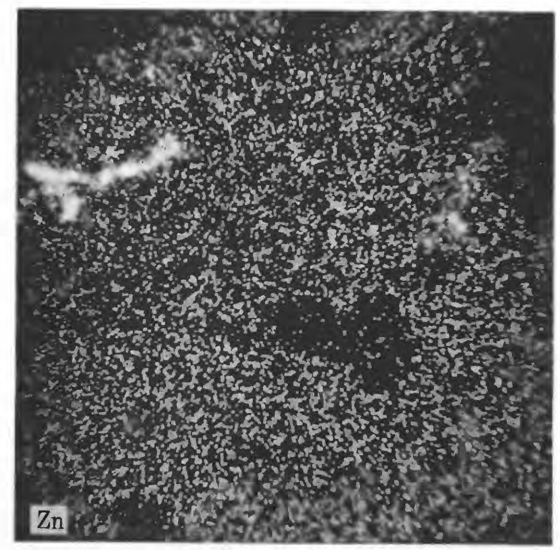

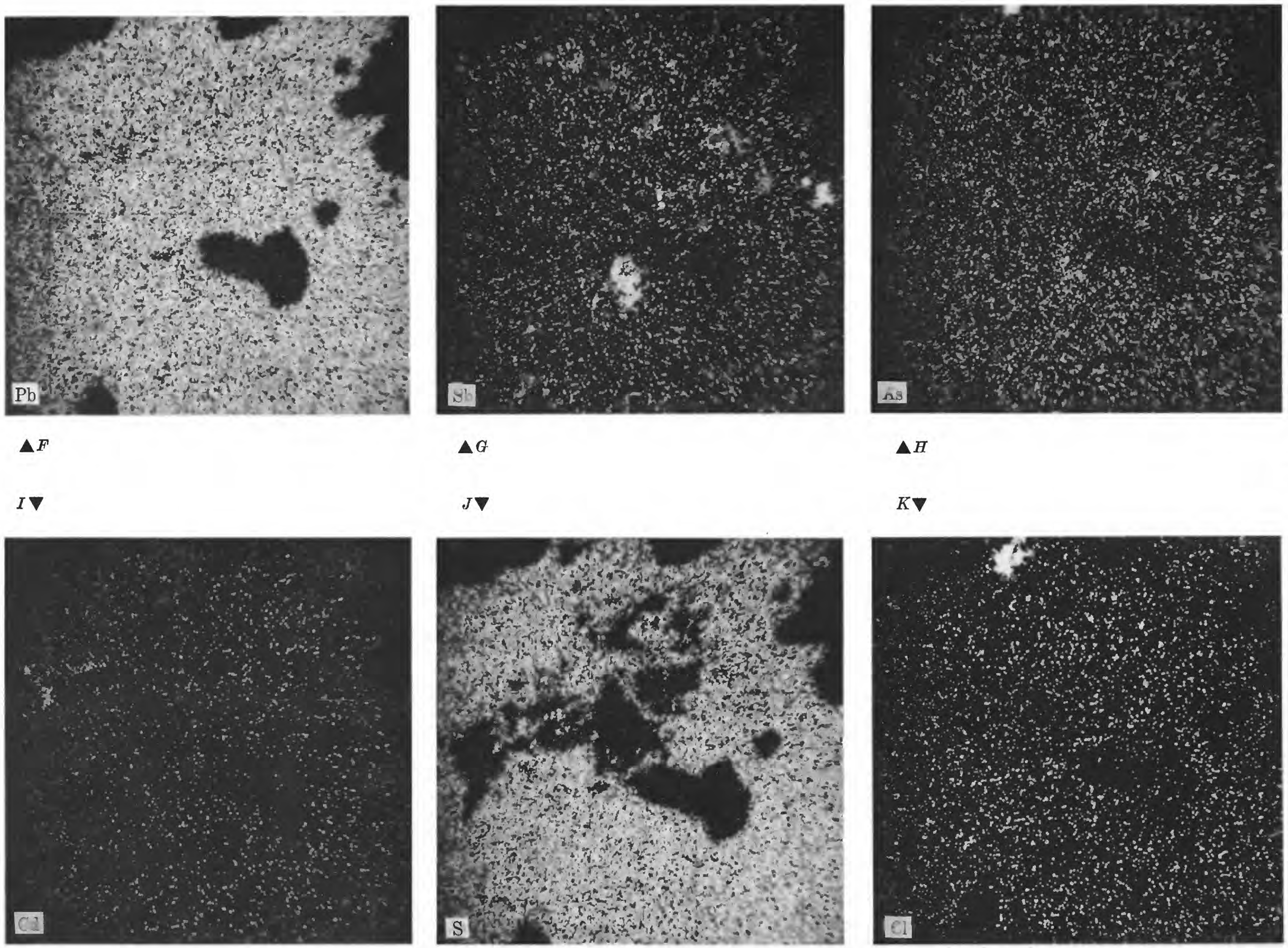

FIGURE 11.—Alteration of galena (Gal) to cerussite (Cer). Note tetrahedrite (Tet) intergrown and locked in galena. Magnification × 645. *A–K*, X-ray scanning images for Si, O, Fe, Cu, Zn, Pb, Sb, As, Cd, S, and Cl in the area outlined in figure 11. The symbols in the lower left-hand corner indicate the element represented by the bright areas of the photograph. Magnification × 400. Several minerals not included in the area shown in figure 11 but shown in X-ray scanning images include mimetite (11*B*, oxygen, *F*, lead, *H*, arsenic, *K*, chlorine), sphalerite (*E*, zinc, *I*, cadmium), and hematite (*B*, oxygen, *C*, iron).

Arsenic.—In contrast to antimony, the concentration of arsenic is low in primary galena ores (table 2). No arsenic sulfides or arsenic-rich sulfosalt minerals were identified. Mimetite has formed near contacts between gangue and galena (fig. 7) and along microfractures in galena (fig. 4). X-ray scanning images for arsenic in corresponding areas are given in figures 4*I* and 7*B*. Concentration of arsenic in mimetite associated with other secondary minerals suggests some migration of arsenic in the ore during oxidation and alteration.

Lead.—Galena is the dominant primary lead mineral in the ore and accounts for more than 95 percent of the total lead in the samples studied. No primary lead-bearing sulfosalt minerals were identified in the galena. The low lead content (<0.04 percent) in tetrahedrite surrounded by galena suggests a very limited solubility for lead in tetrahedrite.

In the sections studied, less than 5 percent of the total lead is in the alteration mineral, cerussite. Alteration of galena to cerussite with remnant inclusions of galena reflects in situ oxidation of the sulfide ore. The apparent tendency for lead sulfide to alter directly to lead carbonate without the formation of lead sulfate suggests that oxidation took place in a slightly acid to alkaline environment with relatively high activity of total carbonate species. (See Eh–pH diagram, Garrels and Christ, 1965, p. 237, 238.)

Zinc.—The dominant part of the zinc in the primary sulfide ore is present as sphalerite, although tetrahedrite, relatively rare in the ore, contains significant amounts of zinc. Zinc in tetrahedrite and sphalerite are shown in X-ray scanning images, figures 4*E* and 11*E*, respectively. Secondary zinc minerals such as smithsonite and hemimorphite were not identified with cerussite and mimetite, even in those areas showing intense alteration. The apparent absence of any zinc carbonate or zinc sulfate species may be explained by their much greater solubility relative to the corresponding lead species.

Cadmium and indium.—Both cadmium and indium are concentrated in the sphalerite of the Burgin ore body. Significant amounts of cadmium, along with large amounts of zinc, are also present in tetrahedrite and reflect the similar geochemical behavior of the two elements. The binary cadmium sulfide, greenockite, was not identified. Indium was identified in sphalerite only. Analysis of secondary minerals associated with both types of galena ore shows no concentration of either cadmium or indium.

Iron.—Iron is low in abundance in both types of galena ore (table 2). This is reflected mineralogically by the very limited amount of pyrite in the ore sample studied. Other iron-bearing minerals, including chalcopyrite and tetrahedrite, are minor in abundance, and the sphalerite is virtually iron free. Secondary minerals coating the samples and filling fractures cutting across them are also virtually iron free. No iron carbonate was found, although small amounts of the iron oxide hematite were identified locally. Small amounts of hematite, closely associated with cerussite, lie just outside the area shown in figure 11. The iron oxide mineral is shown in X-ray scanning images for iron (11*C*) and oxygen (11*B*). Figure 6 shows a photomicrograph of pyrite and chalcopyrite in barite.

SUMMARY AND CONCLUSIONS

The mineralogy of massive galena ores of the Burgin mine in general is deceptively simple, but in detail it presents many complexities. Substantial mineralogical differences exist between the two general types of ore and are reflected in chemical analyses of the bulk ore. The massive coarse-grained type 1 ore is chiefly galena, whereas the massive fine-grained type 2 ore, although dominantly galena, carries significant amounts of sphalerite.

The oxidation and alteration of galena to cerussite along fractures and cleavage directions is well developed in both types of ore. In contrast, sphalerite, identified only in the fine-grained ore, is fresh and unaltered.

Compared with the apparently limited movement and the lack of zinc enrichment in the ore, silver—as a constituent of the obviously secondary or supergene minerals jalpaite and argentite (or acanthite)—is concentrated in, and dispersed through, secondary lead carbonate. Although the amount of silver sulfide-rich cerussite is small compared with the primary galena in the samples studies, more than 50 percent of the total silver content is in this form.

Much of the silver in the primary sulfide ore is in grains of polybasite and tetrahedrite and in smaller amounts of jalpaite dispersed through galena. In many "argentiferous galena" ores the small disseminated inclusions commonly assumed to be "exsolution argentite" probably are actually complex sulfosalt minerals.

The coarsely crystalline "argentiferous galena" contains detectable amounts of silver in the galena, and locally, near the sulfosalt inclusions, there is a notable concentration of the element. In contrast, the fine-grained galena is very low in silver, containing only about one-fifth of the silver found in the coarsely crystalline type. The solubility of silver in galena varies directly with that of antimony.

Only minor amounts of zinc-rich tetrahedrite were found disseminated through galena. That its occurrence is only minor is an advantage, for the presence of larger amounts of the mineral would introduce harmful amounts of zinc and antimony into any lead concentrate produced by flotation milling.

REFERENCES CITED

Adler, I., and Goldstein, J., 1965, Absorption tables for electron probe microanalysis: NASA Tech. Note TND-2984, 276 p.

Bush, J. B., and Cook, D. R., 1960, Bear Creek Mining Company studies and exploration, Pt. 2 *of* The chief oxide-Burgin area discoveries, East Tintic district, Utah; a case history: Econ. Geology, v. 55, no. 7, p. 1507–1540.

Duncumb, P., and Shields, P. K., 1966, Effect of critical excitation potential on the absorption correction, *in* McKinley, T. D., Heinrich, K. F. J., and Wittry, D. B., eds., The electron microprobe, Proceedings of Symposium sponsored by the Electrothermic and Metallurgy Division, The Electrochemical Society, Washington, D. C., 1964: New York, John Wiley & Sons, p. 284–295.

Garrels, R. M., and Christ, C. L., 1965, Solutions, minerals, and equilibria: New York, Harper & Row, 450 p.

Heinrich, K. F. J., 1966, X-ray absorption uncertainty, *in* McKinley, T. D., Heinrich, K. F. J., and Wittry, D. B., eds., The electron microprobe, Proceedings of the Symposium sponsored by the Electrothermic and Metallurgy Division, Electrochemical Society, Washington, D.C., 1964: New York, John Wiley & Sons, Inc., p. 296–377.

Lovering, T. S., and Morris, H. T., 1960, U.S. Geological Survey studies and exploration, Pt. 1 *of* The chief oxide—Burgin area discoveries, East Tintic district, Utah; a case history: Econ. Geology, v. 55, no. 6, p. 1116–1147.

Mining Congress Journal, 1961 [Data on ore content assays]: Mining Cong. Jour., v. 47, no. 4, p. 108.

Palache, Charles, Berman, Harry, and Frondel, Clifford, 1944, Elements, sulphides, sulfosalts, oxides, v. 1 *of* The system of mineralogy of James Dwight Dana and Edward Salisbury Dana [7th ed.]: New York, John Wiley & Sons, Inc., 834 p.

Philibert, J., 1963, A method for calculating the absorption correction in electron probe microanalysis, *in* Pattee, H. H., Cosslett, V. E., and Enstrom, Arne, eds., X-ray optics and X-ray microanalysis, International Symposium on X-ray optics and X-ray microanalysis, 3d, Stanford, Calif., 1962: New York, Academic Press, Inc., p. 379–392.

Skinner, B. J., 1966, The system Cu–Ag–S: Econ. Geology, v. 61, no. 1, p. 1–26.

Taylor, C. M., 1967, Mineralogical applications of the electron-beam microprobe in the study of a gold silver deposit, Knob Hill mine, Republic, Washington: Stanford, Calif., Stanford Univ., Ph. D. thesis.

Taylor, C. M., and Radtke, A. S., 1965, Preparation and polishing of ores and mill products for microscopic examination and electron microprobe analysis: Econ. Geology, v. 60, no. 6, p. 1306–1319.

U.S. GOVERNMENT PRINTING OFFICE: 1969 O—317-359